International Journal of Research (IJR)
e-ISSN: 2348-6848, p- ISSN: 2348-795X Volume 3, Issue 01, January 2016
Available at http://internationaljournalofresearch.org

Adaptive Voltage Control of a 3-Phase Inverter for a Standalone Distributed Generation

V.Chandra sekhar [1] & S.Raj Shekar[2]
[1]M.Tech Scholar, Dept of EEE, A.S.R College of Engineering and Technology, JNTUK, A.P
[2]Assistant Professor, Dept of EEE, A.S.R College of Engineering and Technology, JNTUK, A.P

Abstract:— *Multilevel inverters have received more attentions their considerable advantages such as high power quality, lower harmonic components, better electro- magnetic consistence, lower dv/dt and lower switching losses. Lot of research was going on multi level inverter topologies and many researchers are proposed so many multi level inverter topologies. This paper proposes a robust adaptive voltage control of three-phase voltage source inverter for a distributed generation system in a standalone operation. The proposed adaptive voltage control technique combines an adaption control term and a state feedback control term.*
The proposed algorithm is easy to implement, but it is very robust to system uncertainties and sudden load disturbances. With the proposed system, we can achieve fast transient response, zero steady-state error, and low THD.Mathematical modeling and simulation studies using Simpower systems Block set of MATLAB are proposed. Switching scheme for the proposed converter circuit is designed with the help of sinusoidal pulse width modulation scheme. Total Harmonic distortion in the output voltage is evaluated using FFT tool of MATLAB SIMULINK.

Keywords: Adaptive voltage control; distributed generation system (DGS); robust control; stability analysis; standalone operation; uncertainties; voltage source inverter.

I. INTRODUCTION

Renewable power plants of more than 10 MW in capacity have thereby become a reality [1]. Since 2011, Enercon has been producing the wind turbine E-126/7500 with a power capacity of 7.5 MW [2]. Currently, Sway Turbine and Windtec Solutions are developing 10-MW wind turbine generators, which are expected to be commercially available by 2015 [2]. However, wind farms cover large areas of land. For example, the land area covered by a 3.6-MW turbine can be almost 0.37 km^2, such that 54 turbines would cover about 20 km^2 of land area [1]. Offshore wind farms save land rental expense which is equivalent to 10–18% of the total operating and maintenance costs of a wind farm. Therefore, offshore wind farms have attracted considerable interest in recent years. More than 200 PV power plants have already been installed in the world; each of them generating an output of more than 10 MW. Of these plants, 34 are located in Spain and 26 in Germany. The number of PV power plants will continue to rise. The literature indicates that more than 250 PV power plants will be installed within the next few years. Future PV power plants will have higher power capacity. Indeed, some are to have a capacity in excess of 250 MW. These multi megawatt PV power plants require large areas of land. Owing to this, they are usually installed in remote areas, far from cities. The 20-MW PV power plant in Beneixama, Spain, used about 200 SINVERT 100M inverters and installed approximately 100 000 PV modules in a land area of 500 000 m^2. However, the renewable energy sources have highly variable daily and seasonal patterns, and consumer power demand requirements are also extremely variable in nature. Therefore, it is difficult to operate a stand-alone power system supplied from only one type of renewable energy resource unless there are appropriate energy storage facilities. If enough energy storage capacity is not available, especially in medium- to large-scale systems, a grid-connected renewable power generation may be the only practical solution. For grid integration, a power-frequency transformer operated at 50 or 60 Hz is generally used in the renewable power generation systems to step up the voltage to the grid voltage levels of 6–36 kV, which results in high capital and installation costs because of its heavy weight and large size. For example, the weight and volume of a

0.69/33 kV, 2.6-MVA transformer is typically in the range of 6–8 t and 5- 9 m^3, respectively. A liquid-filled 2-MVA step-up transformer uses about 900 kg of liquid as the coolant and insulator, which requires regular monitoring and replacement. These levels are critical in offshore and remote area applications, where the cost of installation and regular maintenance is extremely high. In an offshore wind farm, this transformer is usually installed at a height of about 80 m inside the nacelle together with other equipment such as the generator and power converter. This heavy and large step-up transformer significantly increases the weight and volume of the nacelle as well as increasing the mechanical stress of the tower. For example, the foundation size of a 2.3-MW wind turbine is 314 m^2 and the approximate weight is 2000 t or more. The installation cost of an offshore wind farm is, on average, approximately 20% of the capital cost.

With the arrival of new high-power semiconductor devices, new power converter structures are conceived to meet the needs of future medium- or high-voltage converter systems. In this highly active area, the modular multilevel cascaded (MMC) converter topologies and circuits have attracted a high degree of attention for their application in medium- and high-voltage systems [3]–[4]. The component numbers of the MMC converters scale linearly with the number of levels, and individual modules are identical and modular in construction thereby enabling high level number attainability [8]. Furthermore, in the case of a fault in one of these modules, it is possible to replace it quickly and easily. However, the MMC converter requires multiple-isolated dc sources that must be balanced [2]–[3]. Accordingly, its application is not straightforward, especially in renewable power generation systems.

Recently, an adaptive control method has been widely considered in the standalone DGS or UPS voltage control. In [4] and [5], the precise voltage tracking is achieved under distorting loads by using the adaptive control for the output voltage based on the ideas of dissipativity. In these papers, the uncertainties in the system parameters are addressed through the adaptation, and the stability of the system is guaranteed even under system parameters variations. However, the major drawback of these techniques is the computation complexity. In order to reduce this complexity, a certain predefined value for the parameters is required. In [6], an adaptive output voltage controller based on the resonant harmonic filters, which measures the capacitor current and the load currents in the same sensor, is proposed in order to compensate for the unbalance and harmonic distortion on the load. The adaptation law is also included to cope with the uncertainties in the system parameters. However, the information about output voltage THD is not presented so it is not easy to evaluate the quality of the controllers. In [7], an adaptive control method based on the proportional-derivative control technique is presented for a pulse width modulation (PWM) inverter operation in an islanded DGS. This paper can guarantee good voltage regulation under various operating conditions such as sudden load changes, unbalanced load, and nonlinear load. However, it is not an easy task to choose the appropriate control gains according to the design procedure mentioned in the paper.

II. PROPOSED TOPOLOGY AND IT'S OPERATION

A. State-Space Model of a Load-Side Inverter :

Fig. 1 describes a block diagram of a standalone DGS using renewable energy sources which are wind turbines, solar cells, fuel cells, etc. As depicted in Fig. 1, the DGS is divided into six parts: an energy source, an ac–dc power converter (wind turbines) or a dc–dc boost converter (solar cells or fuel cells), a three-phase dc–ac inverter, an *LC* output filter, an isolation transformer, and a local load. In this paper, a renewable energy source and an ac–dc power converter or a dc–dc boost converter can be replaced by a stiff dc voltage source (Vdc) because this paper focuses on designing a robust adaptive voltage controller under various types of loads such as balanced load, unbalanced load, and nonlinear load. Also, this representation can be acceptable because the front converter (i.e., an ac–dc power converter or a dc–dc boost converter) can rapidly recover the reduced dc-link voltage when a heavy load is suddenly applied. The DG energy sources usually work together with energy storage devices (e.g., batteries, flywheels, etc.) in order to back up the DS systems during the transient, and increase the power quality and reliability. Furthermore, the isolation transformer is not used to reduce cost and volume assuming that the customers need a low voltage ac source (below 600 V) which the DGSs using renewable energy sources can generate without the help of the transformer.

Fig. 2 shows a schematic diagram of a three-phase dc–ac inverter with an *LC* filter in a standalone application. In this figure, it consists of a dc voltage source (*V*dc), a three phase inverter (*S*1 to *S6*), an output filter (*Lf* and *Cf*), and a three-phase resistive load (*RL*). The *LC* output filter is an indispensable part in this circuit because it plays a role in eliminating harmonic components of the inverter output voltage caused by high-frequency switching actions.

LC Filter values and all the remaining calculated parameters values are given in Appendix section .

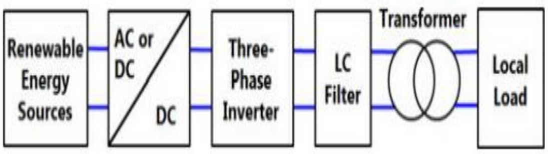

Fig.1. Block diagram of a standalone DGS using renewable energy sources.

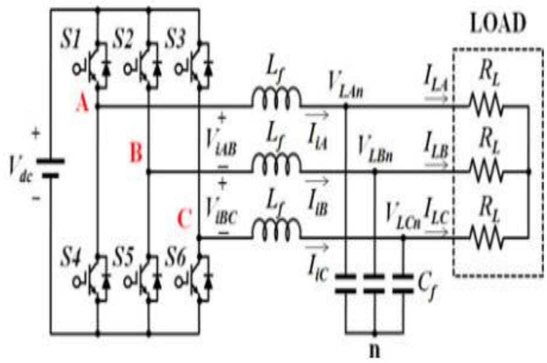

Fig.2. Schematic diagram of a three-phase dc to ac inverter with an *LC* filter in a standalone application

B. Block diagram of proposed system and its principle operation :

Fig.3 shows the block diagram of the proposed adaptive voltage controller based on the fallowing two equation.

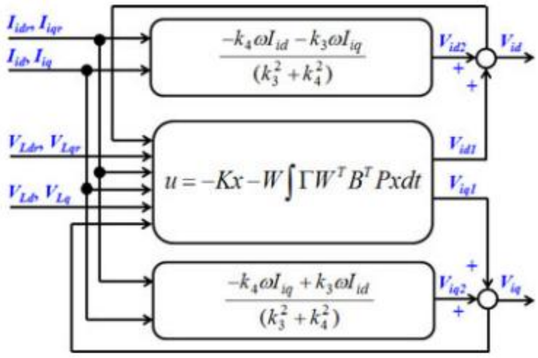

Fig. 3. Block diagram of the proposed adaptive voltage controller

$$\begin{cases} V_{id2} = \dfrac{-k_4 \omega I_{id} - k_3 \omega I_{iq}}{(k_3^2 + k_4^2)} \\ V_{iq2} = \dfrac{-k_4 \omega I_{iq} + k_3 \omega I_{id}}{(k_3^2 + k_4^2)} \end{cases} .$$

In this paper, a prototype 450VA DG unit is considered to implement the proposed control algorithm. Table I gives the nominal parameters for simulations and experiments.

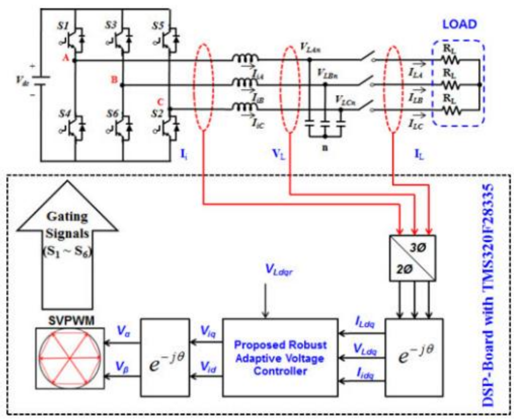

Fig. 4. Block diagram of the proposed adaptive voltage control system

Fig. 4 shows the block diagram of the proposed adaptive voltage control system. As illustrated in Fig. 4, the inverter phase currents (**I***i*), load output voltages (**V**$_L$), and load phase currents (**I**$_L$) are measured and then are transformed to the quantities ($\mathbf{I}_{idq}$, $\mathbf{V}L_{dq}$, $\mathbf{I}L_{dq}$) in the synchronously rotating *d*–*q* reference frame, respectively. In this paper, a space-vector PWM technique is chosen to

International Journal of Research (IJR)
e-ISSN: 2348-6848, p- ISSN: 2348-795X Volume 3, Issue 01, January 2016
Available at http://internationaljournalofresearch.org

implement the control inputs (*Vid* and *V iq*) that the proposed voltage controller generates in real time.

In the paper, simulations and experiments are carried out to verify the effectiveness of the proposed adaptive control algorithm under the following four conditions:
Balanced load (0% →100%): The balanced resistive load is instantaneously applied to the inverter output terminals.

2) Balanced load (100% → 0%): The balanced resistive load is instantaneously removed from the inverter output terminals

3) Unbalanced load: The unbalanced resistive load is connected to the inverter output terminals, i.e., only phase *C* is opened
4) Nonlinear load: A three-phase full-bridge diode rectifier is connected to the inverter output terminals.

III. MATLAB BASED SIMULATION & IT'S RESULTS

Fig.5. & Fig.6 shows the MATLAB based simulation diagram of proposed system.

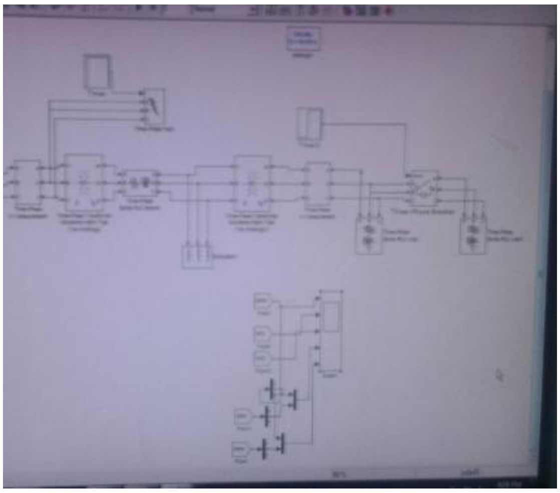

Fig.5. MATLAB based simulation diagram of proposed system with masked blocks

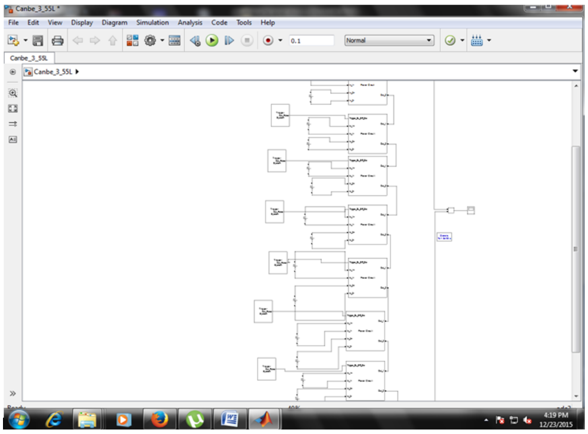

Fig.6. MATLAB based simulation diagram with inner blocks of proposed system

Fig.7. shows the MATLAB based simulation waveform diagram of proposed system with proposed adaptive voltage controller with 150% uncertainties of system parameters

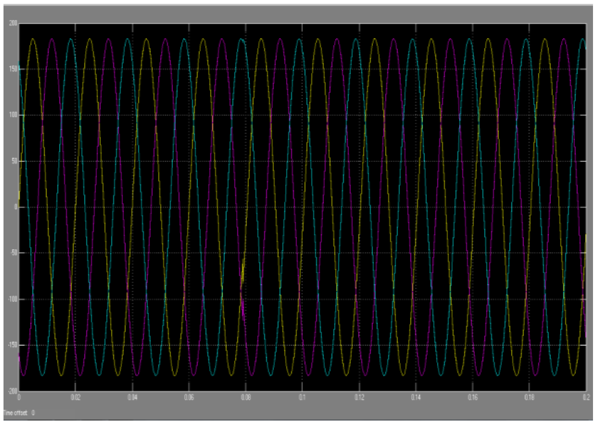

Fig.7. MATLAB based simulation waveform diagram of proposed system - Balanced resistive load

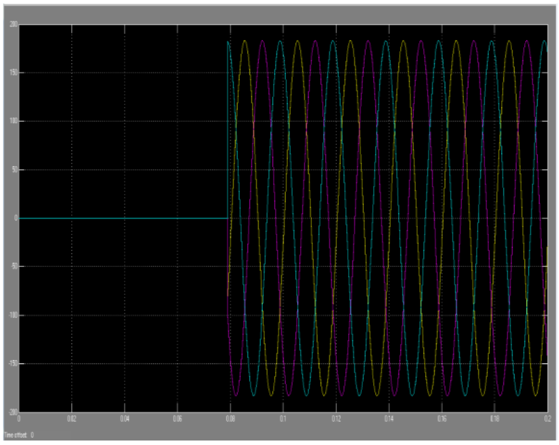

Fig.8. MATLAB based simulation waveform diagram of proposed system - Balanced resistive load

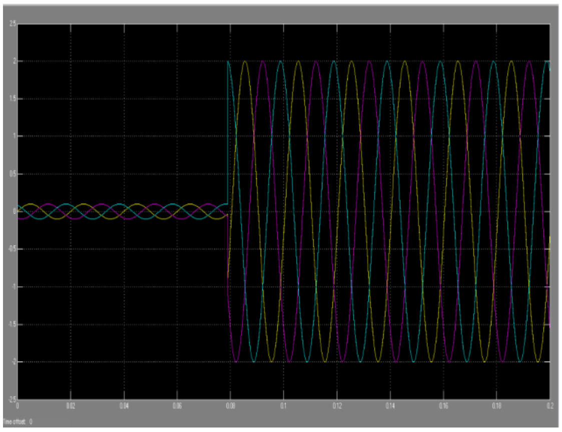

Fig.9. MATLAB based simulation waveform diagram of proposed system - Unbalanced resistive load

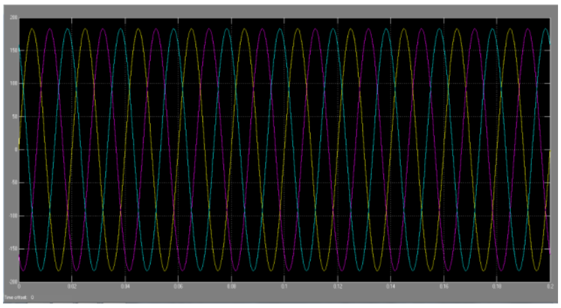

Fig.10. Simulation results of the non adaptive voltage controller with uncertainties of system under a nonlinear load – Load voltage

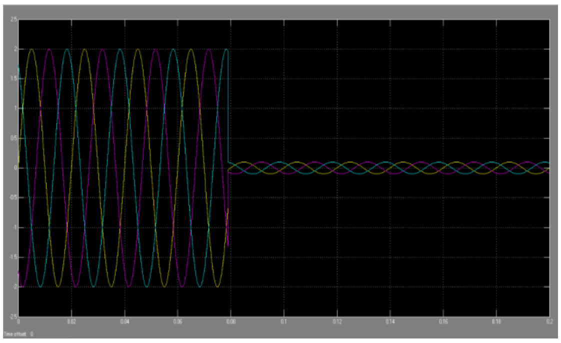

Fig.11. Simulation results of proposed adaptive voltage controller with uncertain Simulation results ties of system parameters under a balanced resistive load - Load phase currents ($\mathbf{I}_L$)

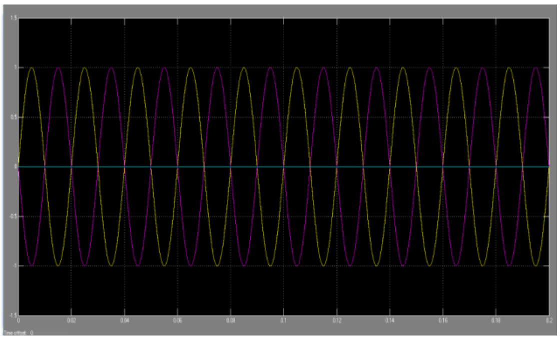

Fig.12. Simulation results of proposed adaptive voltage controller uncertainties of system parameters under a nonlinear load- Load phase currents ($\mathbf{I}_L$) and inverter phase currents

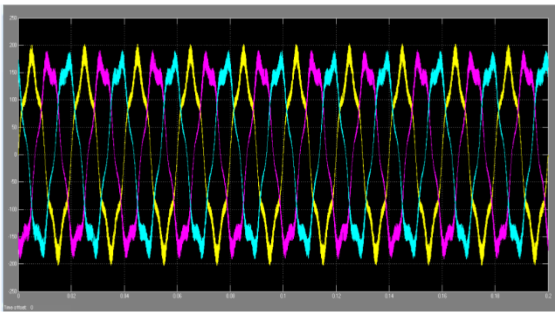

Fig.13. Simulation results of the non adaptive voltage controller with uncertainties of system parameters under a nonlinear- Load phase currents ($\mathbf{I}_L$) and inverter phase currents ($\mathbf{I}i$).

APPENDIX TABLE .I.SIMULATION SPECIFICATIONS

Parameter	***Rating***
R	R = 80 Ω
LC Filters	L = 10 mH , 6μF
Output frequency	60 Hz
DC Link Voltage	280V
Maximum output voltage	110 V
Non Linear Load	C=3300 μF , R=500 Ω

IV. Conclusion & Future Scope

In the paper, simulations and experiments are carried out to verify the effectiveness of the proposed adaptive control algorithm is presented. Fig.7-Fig.13 shows the simulation results of the proposed adaptive voltage controller using Matlab/Simulink under four different conditions. The experimental results of the non adaptive voltage controller under the nonlinear load. The transient and steady-state performances are good with fast transient responses and small steady-state errors. It can be obviously observed from the simulation and experimental results that the proposed adaptive voltage control method achieves better voltage tracking performance (i.e., smaller steady-state error and lower THD) under various types of loads (i.e., balanced load, unbalanced load, and nonlinear load) than the corresponding non adaptive control method even though there exist uncertainties of system parameters. Finally, the simulation and experimental results have demonstrated that the proposed control scheme gives satisfactory voltage regulation performance such as fast dynamic behavior, small steady-state error, and low THD under various loads (i.e., no load, balanced load, unbalanced load, and nonlinear load) in the presence of the uncertainties of system parameters.

References

[1] H. K. Kang, C. H. Yoo, I. Y. Chung, D. J. Won, and S. I. Moon, “Intelligent coordination method of multiple distributed resources for harmonic current compensation in a microgrid,” *J. Elect. Eng. Technol.*, vol. 7, no. 6, pp. 834–844, Nov. 2012.

[2] M. Liserre, T. Sauter, and J. Y. Hung, “Future energy systems: Integrating renewable energy sources into the smart power grid through industrial electronics,” *IEEE Ind. Electron. Mag.*, vol. 4, no. 1, pp. 18–37, Mar. 2010.

[3] M. Y. Kim, Y. U. Song, and K. H. Kim, “The advanced voltage regulation method for ULTC in distribution systems with DG,” *J. Elect. Eng. Technol.*, vol. 8, no. 4, pp. 737–743, Jul. 2013.

[4] T. D. Do, V. Q. Leu, Y. S. Choi, H. H. Choi, and J. W. Jung, “An adaptive voltage control strategy of three-phase inverter for stand-alone distributed generation systems,” *IEEE Trans. Ind. Electron.*, vol. 60, no. 12, pp. 5660– 5672, Dec. 2013.

[5] M. B. Delghavi and A. Yazdani, “An adaptive feedforward compensation for stability enhancement in droop-controlled inverter-based microgrids,” *IEEE Trans. Power Del.*, vol. 26, no. 3, pp. 1764–1773, Jul. 2011.

[6] M. B. Delghavi and A. Yazdani, “Islanded mode control of electronically coupled distributed-resource units under unbalanced and nonlinear load conditions,” *IEEE Trans. Power Del.*, vol. 26, no. 2, pp. 661–673, Apr. 2011.

[7] Ebrahim Babaei,Sara Laali, and Somayeh Alilu, “Cascaded Multilevel Inverter With Series Connection of Novel H-Bridge Basic Units”, IEEE Transctions on Industrial Electronics , Vol.61 , No.12 , December 2014 , pp. 6664-6671

[8] S. Laali, K. Abbaszades, and H. Lesani, “New hybrid control methods based on multi-carrier PWM techniques and charge balance control methods for cascaded multilevel converters,” in *Proc. CCECE*, 2011 pp. 243–246.

[9] J. Napoles, A. J. Watson, and J. J. Padilla, “Selective harmonic mitigation technique for cascaded H-bridge converter with nonequal dc link voltages,” *IEEE Trans. Ind. Electron.*, vol. 60, no. 5, pp. 1963–1971, May 2013.

[10] N. Farokhnia, S. H. Fathi, N. Yousefpoor, and M. K. Bakhshizadeh, “Minimisation of total harmonic distortion in a cascaded multilevel inverter by regulating of voltages dc sources,” *IET Power Electron.*, vol. 5, no. 1, pp. 106–114, Jan. 2012.

[11] Welflen Ricardo Nogueira Santos , Edison Roberto Cabral da Silva and Cursino Brandao Jacobina , “The Transformerless Single-Phase Universal Active Power Filter for Harmonic and Reactive Power Compensation”, IEEE Transactions on Power Vol.29 , No.7 , pp. 3563- 3572 July 2014

[12] Y. Tang, P. C. Loh, P. Wang, F. H. Choo, F. Gao, and F. Blaabjerg, “Generalized design of high performance shunt active power filter with output lcl filter,” *IEEE Trans. Ind. Electron.*, vol. 59, no. 3, pp. 1443–1452, Mar. 2012

[13] E. Babaei, S. Alilu, and S. Laali, “A new general topology for cascaded multilevel inverters with reduced number of components based on developed H-bridge,” *IEEE Trans. Ind. Electron.*,

vol. 61, no. 8, pp. 3932–3939, Aug. 2014.

[14] J. Ebrahimi, E. Babaei, and G. B. Gharehpetian, "A new topology of cascaded multilevel converters with reduced number of components for high-voltage applications," *IEEE Trans. Power Electron.*, vol. 26, no. 11, pp. 3119–3130, Nov. 2011.

[15] Q.-N. Trinh and H.-H. Lee, "An advanced current control strategy for three-phase shunt active power filters," *IEEE Trans. Ind. Electron.*, vol. 60, no. 12, pp. 5400–5410, Dec. 2013.

[16] S. Laali, K. Abbaszades, and H. Lesani, "A new algorithm to determine the magnitudes of dc voltage sources in asymmetrical cascaded multilevel converters capable of using charge balance control methods," in *Proc. ICEMS*, Incheon, Korea, 2010, pp. 56–61.

[17] M. F. Kangarlu and E. Babaei, "A generalized cascaded multilevel inverter using series connection of sub-multilevel inverters," *IEEE Trans. Power Electron.*, vol. 28, no. 2, pp. 625–636, Feb. 2013.

[18] J. Pereda and J. Dixon, "Cascaded multilevel converters: Optimal asymmetries and floating capacitor control," *IEEE Trans. Ind. Electron.*, vol. 60, no. 11, pp. 4784–4793, Nov. 2013.

[19] E. Babaei, M. Farhadi Kangarlu, and F. Najaty Mazgar, "Symmetric and asymmetric multilevel inverter topologies with reduced switching devices," *Elect. Power Syst. Res.*, vol. 86, pp. 122–130, May 2012.

[20] I. Vechiu, O. Curea, and H. Camblong, "Transient operation of a four-leg inverter for autonomous applications with unbalanced load," *IEEE Trans. Power Electron.*, vol. 25, no. 2, pp. 399–407, Feb. 2010.

[21] J. He and Y. W. Li, "An enhanced microgrid load demand sharing strategy," *IEEE Trans. Power Electron.*, vol. 27, no. 9, pp. 3984 3995, Sep. 2012.